HIGH MASS STAR FORMATION IN THE GALAXY[1]

N87-24267

N.Z. Scoville
Astronomy Department 105-24
California Institute of Technology
Pasadena, CA 91125

J.C. Good
Infrared Processing and Analysis
Center 100-22
Pasadena, CA 91125

ABSTRACT. The Galactic distributions of HI, H_2 and HII regions are reviewed in order to elucidate the high mass star formation occurring in galactic spiral arms and in active galactic nuclei. Comparison of the large scale distributions of H_2 gas and radio HII regions reveals that the rate of formation of OB stars depends on $\langle n_{H_2} \rangle^{1.9}$ where $\langle n_{H_2} \rangle$ is the local mean density of H_2 averaged over 300 pc scale lengths. In addition the efficiency of high mass star formation (per unit mass of H_2) is a decreasing function of cloud mass in the range 2×10^5 - 3×10^6 M_o. These results suggest that high mass star formation in the galactic disk is initiated by cloud-cloud collisions which are more frequent in the spiral arms due to orbit crowding. Cloud-cloud collisions may also be responsible for high rates of OB star formation in interacting galaxies and galactic nuclei.

Based on analysis of the IRAS and CO data for selected GMCs in the Galaxy, the ratio L_{IR}/M_{H_2} can be as high as 30 L_o/M_o for GMCs associated with HII regions. This is a factor of ten higher than the mean value of 2.75 L_o/M_o for the H_2 in the galactic disk. The total far infrared luminosity at λ=1-500 μm associated with the molecular disk in the Milky Way is 6×10^9 L_o. The L_{IR}/M_{H_2} ratios and dust temperature obtained in many of the high luminosity IRAS galaxies are similar to those encountered in galactic GMCs with OB star formation. High mass star formation is therefore a viable (but certainly not unique) explanation for the high infrared luminosity of these galaxies.

---

1. Throughout this article, we have scaled all derived parameters to the new Sun-Galactic center distance R_o=8.5 kpc.

1. INTRODUCTION

Star formation is central to our understanding of both the structural evolution of galaxies and their energetics. The formation of high mass stars is a key element in both the spiral structure of galaxies and the highly luminous galactic nuclei since in both instances, rapid, OB star formation has been proposed as an efficient mechanism for generating a high luminosity with a small expenditure of interstellar gas. Although massive star formation is often invoked to account for the enormous energy output of extragalactic nuclei, the underlying cause for the bias toward high mass stars is not at all understood.

In this contribution, we review the results of several recent investigations specifically designed to elucidate the formation of OB stars in the Galaxy. These studies also provide us with the diagnostics needed to distinguish high and low mass star formation in external galaxies.

Carol J. Lonsdale Persson (Editor)
Star Formation in Galaxies

2. GENERAL CONSIDERATIONS

Numerous millimeter and infrared studies of nearby star formation regions have demonstrated that virtually all star formation activity in the Milky Way occurs within molecular (not atomic) hydrogen clouds. The bulk of the molecular gas is contained in giant molecular clouds (GMCs) of mass 10^5-10^6 M_o. For a GMC of diameter 40 pc, the mean internal density is $\sim$200 H_2 cm^{-3} (see Scoville and Sanders 1986 for a review).

The total mass of molecular gas in the Milky Way is estimated to be approximately 2.3×10^9 M_o based on CO line surveys of the inner galaxy. The maximum global star formation rate for the Milky Way would be 10^3 M_o yr^{-1} if these clouds were undergoing free-fall collapse ($\tau_{ff}=3 \times 10^6$ years for a density of 200 cm^{-3}). Since the actual star formation rate is estimated to be approximately 5 M_o yr^{-1}, it is immediately apparent that the GMCs are generally stable against collapse. That is, the overall efficiency for star formation on the free fall collapse time is <1%. We should therefore view the gas parcels within the molecular clouds as being in an "inactive" state 99% of the time; only occasionally (presumably by unusual circumstances) are they activated to collapse and form stars.

Two alternative viewpoints can be taken with regard to star formation mechanisms. On the one hand, we may picture star formation as a percolation process, ie. once the clouds form, star formation proceeds inevitably, albeit at a slow rate. In this picture, the overall star formation rate within any region of the galaxy should vary linearly with the total mass of molecular gas. A second possibility is that external, environmental factors occasionally initiate the star formation at a high efficiency for a short time. For example, the shocks associated with galactic spiral arms, expanding HII regions (Elmegreen and Lada 1977) or supernovae remnants (Herbst and Assousa 1977) have been proposed as the initiation mechanism of high mass star formation on cloud surfaces. A fourth mechanism (not discussed much in recent years but for which we believe there is considerable observational support) is the compression of molecular gas in the interface between colliding GMCs. This latter process is consistent with observed concentration of high mass stars in the spiral arms where the cloud-cloud collision frequency is highest (due to orbit crowding in the spiral arms) and with observations of the star formation efficiency as a function of cloud mass (see below).

3. THE LARGE SCALE DISTRIBUTION OF MOLECULES

The most striking characteristic of the molecular gas distribution in the galaxy is the existence of a ring-like maximum midway between the Sun and the galactic center. This feature (at R=3-7 kpc), containing 75% of the total molecular gas, was first identified in the early survey of Scoville and Solomon (1975) and it has been confirmed by all subsequent CO emission surveys (eg. Burton et al 1975, Cohen et al 1980, Robinson et al 1984, and Sanders, Solomon and Scoville 1984).

In Figure 1, we show the galactic radial distribution of molecular gas derived from the 40,000 point Massachusetts-Stony Brook CO survey in the first galactic quadrant (Clemens, Sanders, and Scoville 1986). For comparison the distributions of radio HII regions and atomic hydrogen are also shown. The ring-like distribution seen in both the molecular hydrogen and the HII regions, is totally absent in HI (which has a relatively flat distribution outside R=3

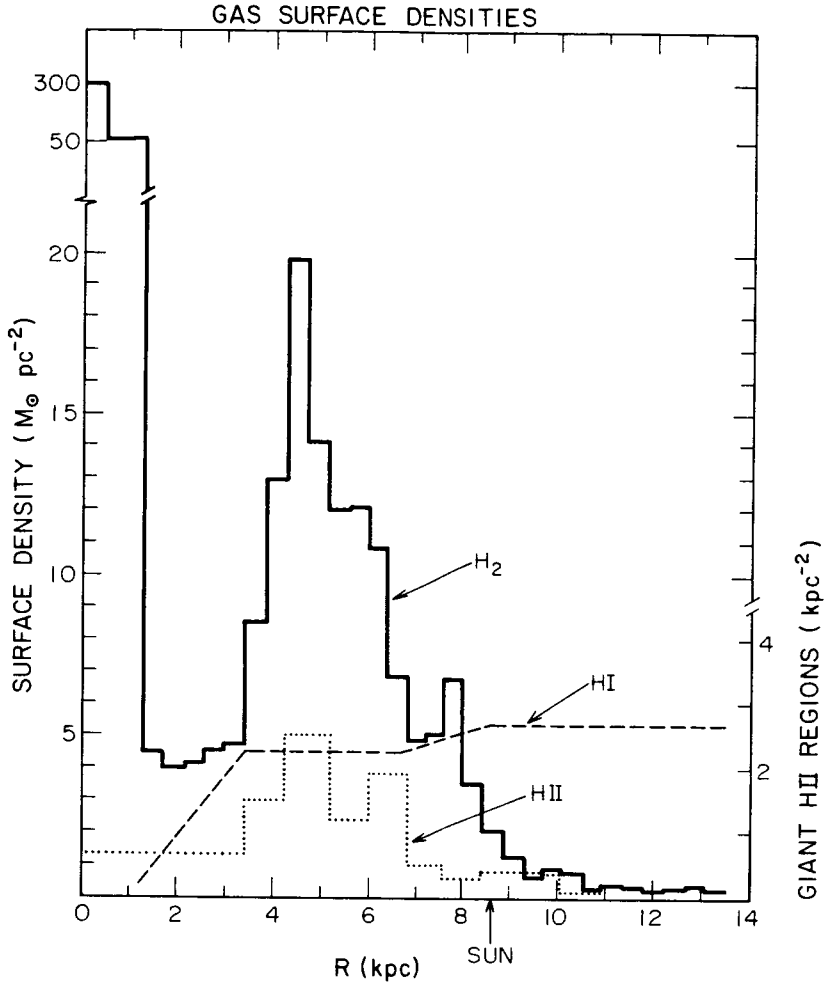

Figure 1. Comparison of the H_2, HI, and giant HII regions surface densities in the Galaxy. Values for H_2 and HI include a 1.36 correction for He. The HI distribution is from Burton and Gordon (1978) and the H_2 from Clemens, Sanders, and Scoville (1986) and corrected to R_o=8.5 kpc.

kpc and a hole in the central region). A second major feature of the molecular gas distribution is the sharp peak within 400 pc of the galactic center. The total mass of molecular gas within the galactic center peak and the molecular cloud ring at 3-7 kpc are 2×10^8 M_o and 1.8×10^9 M_o, respectively. The total H_2 and HI masses at R<14 kpc are each $\sim2.3\times10^9$ M_o (assuming R_o=8.5 kpc, cf. Scoville and Sanders 1986). The Z distributions of molecular gas and HII regions are also very similar with the thickness (FWHM) of approximately 90 pc in the area of the molecular ring, whereas the diffuse atomic hydrogen has approximately twice this scale height.

Although all investigators using CO to survey the large scale distribution of molecular clouds agree that there are large concentrations of CO emission corresponding to the tangential directions (l=32 and 50°) of the inner spiral arms, there is still controversy concerning the density contrast between the arm and inter-arm regions. For example, Sanders (1981) estimates an arm-interarm

contrast of approximately 3:1 averaged over length scales of 500 pc, yet Cohen et al (1980) assert that virtually all giant molecular clouds are confined to the arms. The principle reasons for this disagreement are the loose definition of the spiral arm locations and widths and uncertainities in the distances assigned to emission features due to the two-fold ambiguity in the kinematic distance and the finite velocity dispersion of the clouds.

Perhaps the best approach to the spiral arm question is to appeal to high resolution observations in nearby external galaxies similar to the Milky Way. In this spirit, it is significant that Rydbeck et al (1985) find only a 20% enhancement in the molecular emission along the spiral arms in M51 as compared with the mean emission at each radius when averaged over a length of approximately 1 kpc. In M83, Allen, Atherton and Tilanus (1986) found the HI emission peaks downstream from the dust lanes and they point out that the absence of HI emission from either the dust lanes themselves or the upstream side of the spiral arms implies that the interarm gas must be largely molecular. The latter investigation didn't provide a quantitative estimate of the density contrast, but it does at least clearly settle the issue of whether molecular clouds can occur outside of the spiral arms.

Within the Milky Way (at R=3-7 kpc), all the observations are consistent with at least 50% of the molecular gas being in interarm regions and a density contrast of >3:1. The interarm gas fraction could be even higher if a tight definition is adopted for the spiral arms. The much greater arm-interarm contrast seen in the galactic HII regions then implies that the spiral arm clouds are either intrinsically different in a way which favors high mass star formation or that OB star formation is induced by environmental factors such as galactic spiral shocks or cloud-cloud collisions (which are more frequent in the arms).

4. GMCS ASSOCIATED WITH HIGH MASS STAR FORMATION

We have recently undertaken a comparative study of discrete CO emission regions from the Massachusetts/Stony Brook galactic CO survey (Sanders et al 1986) and radio HII regions. From the CO survey, we have compiled three samples of giant molecular clouds (Scoville et al 1986). The first sample, which we take to be the general cloud population, contains 1,427 emission regions with CO temperatures exceeding 5 K. A second sample, which is a subset of the first, contains 255 hot CO emission cores (delineated at the 9 K level). The cloud cores are regions of molecular gas subject to strong heating--presumably active, star forming gas. The third sample of GMCs consists of 95 clouds associated with 171 radio HII regions (Downes et al 1980 and Lockman 1986).

4.1 Correlation of Hot Cloud Cores with Spiral Arms

Not surprisingly, the clouds associated with HII regions appear significantly hotter than the general cloud population. The mean peak CO temperature within the HII region clouds is 11.4 K while that in the general cloud population is 7.4 K. This correlation between hot molecular clouds and the spiral arm HII regions has been pointed out by Sanders, Scoville, and Solomon (1985), Solomon, Sanders and Rivolo (1985), and Scoville et al (1985).

The longitude-velocity distributions of the three cloud samples are shown

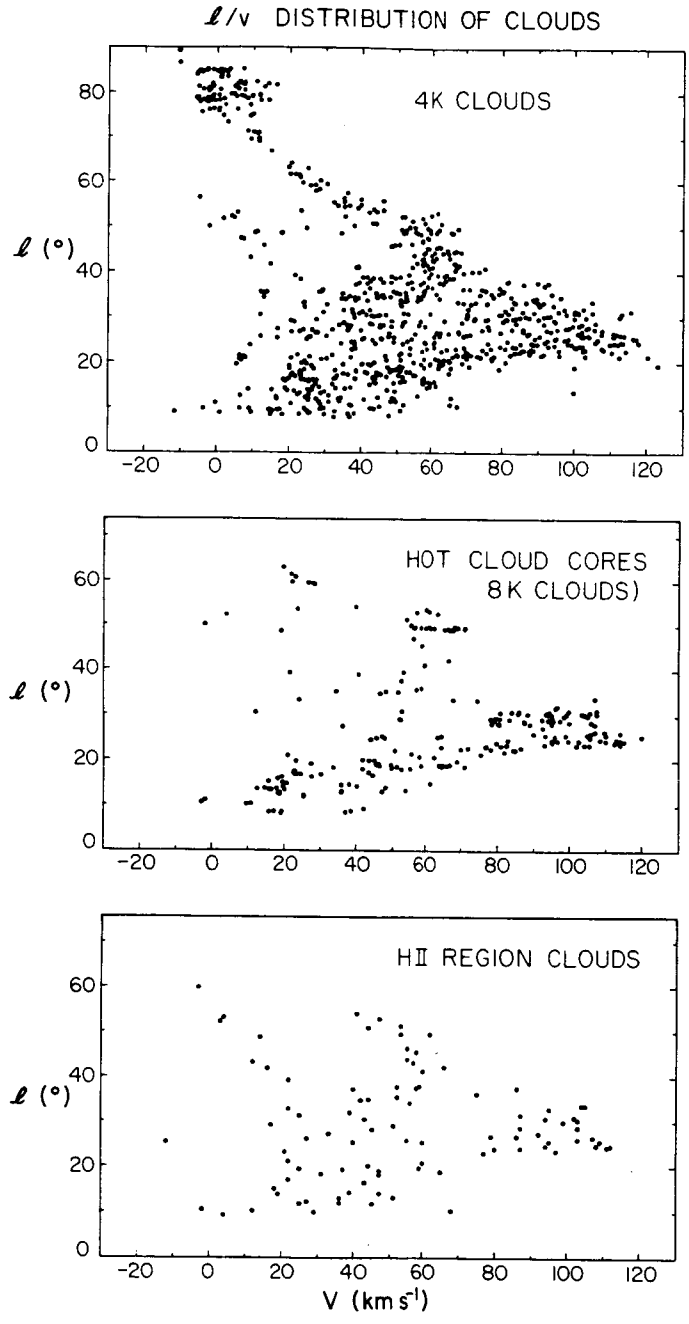

Figure 2. The longitude-velocity distribution of the general cloud population in the first galactic quadrant is contrasted with that of hot cloud cores and clouds associated with HII regions (Scoville et al 1986).

in Figure 2. There it can be seen that the hot cloud cores and HII region clouds exhibit a much tighter confinement within the longitude-velocity plane than the general cloud population. Indeed, the hot cloud cores appear to fall along two arcs stretching from l=0°, V=0 km s^{-1} to the terminal velocities at l=32 and 50° -- the Scutum and Sagittarius arms.

The tight confinement of hot cloud cores to the spiral arms does not address the fundamental question of why the OB star formation favors the GMCs in the spiral arms since clouds undergoing massive star formation will have higher temperatures due to the presence of the luminous embedded stars.

4.2 The Decreasing Efficiency of OB Star Formation in Massive GMCs

The more interesting question is whether the spiral arm clouds are intrinsically different (eg. have a different mass spectrum or internal density) than the more widely distributed disk population clouds. It is therefore of interest to note that the mean diameter of the HII region clouds (at the 4 K CO boundary) is 52 pc, effectively a factor of two larger than that of the general GMC population measured at the same threshold temperature (Scoville et al 1986). Although it is clear that massive star formation tends to prefer the larger GMCs, this may simply reflect the greater mass and therefore, the larger number of sites for star formation in the larger clouds.

In order to analyze the efficiency (per unit mass of H_2) for massive star formation in clouds of varying mass, we show in Figure 3 the HII region free-free luminosity normalized by the cloud mass for clouds in five mass bins between $2x10^5$ and $3x10^6$ $M_\odot$. Also shown is the normalized number of giant HII regions as a function of cloud mass. The figure demonstrates that the efficiency (per unit mass of H_2) for both uv emission and formation of separate OB star clusters decreases for high mass clouds compared to lower mass clouds over this mass range. Thus, the formation rate for massive stars is not simply proportional to the total mass of H_2, but must depend on other factors such as the galactic location or the internal properties of the clouds.

The decreasing efficiency for OB star formation in higher mass clouds argues rather strongly against mechanisms involving internal stimulation of the clouds to initiate star formation. This is because an internal stimulation process should generally have a higher efficiency in more massive clouds where there is more material (surrounding the trigger) ready to be stimulated. For this reason, sequential star formation models such as the compression of shells at the edges of HII regions (Elmegreen and Lada 1977) do not appear to dominate in the formation of massive stars.

4.3 Cloud-Cloud Collisions to Form OB Stars

An alternative mechanism for forming massive stars is the compression of gas in the interface between colliding clouds and cloud clumps (cf. Scoville, Sanders, and Clemens 1986). This mechanism is strongly supported by comparison of the galactic distributions of molecular clouds and HII regions. Recently, Clemens et al (1986) have analyzed the Massachusetts-Stony Brook CO survey to yield an approximate face-on distribution for the molecular gas in the inner galaxy using scale height information to resolve the distance ambiguities.

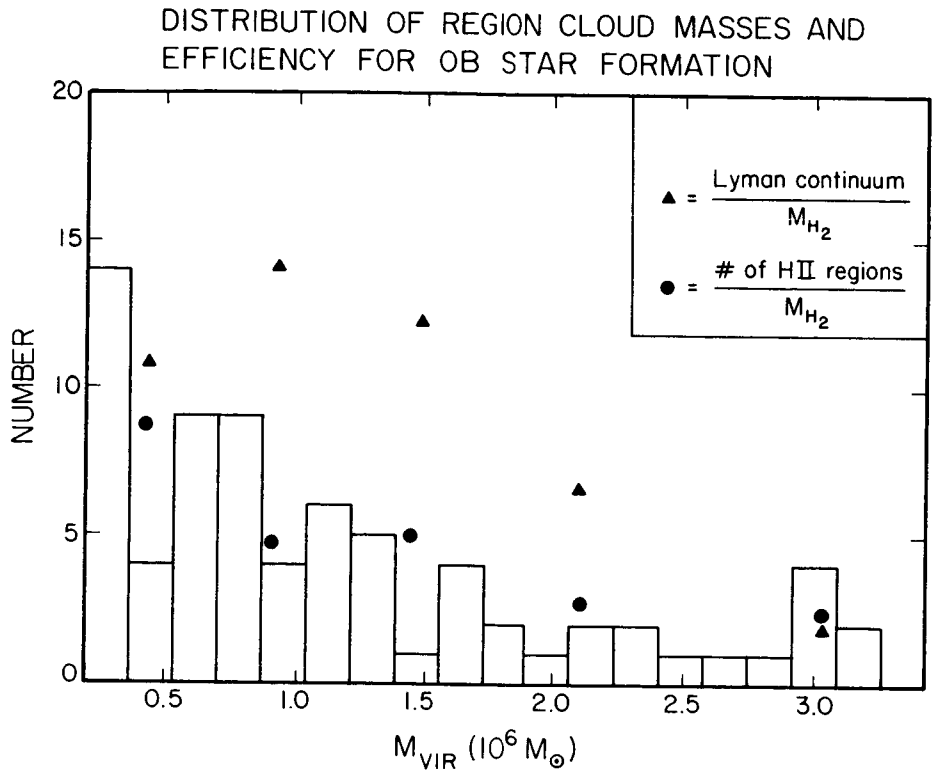

Figure 3. The distribution of virial masses and OB star formation efficiencies (per unit mass of H_2) are shown for 71 GMCs with associated HII regions at known distances (Scoville et al 1986).

Figure 4 shows the dependence of the number of HII regions on the molecular hydrogen density averaged over length scales of ∿300 pc. The best fit power law is

$$N_{HII} \propto \langle n_{H_2} \rangle^{1.9\pm0.2} \quad .$$

The quadratic dependence of the HII region density (presumably the OB star formation rate) on the molecular hydrogen density is strongly suggestive that OB stars form as a result of a collision process, such as cloud-cloud collisions.

Since the 4 km s^{-1} rms velocity dispersion of giant molecular clouds (Clemens 1985) is comparable to or less than the typical internal velocities in the clouds, it is clear that most collisions between GMCs will result in a bound complex rather than disruption of the clouds. During a cloud-cloud collision, the interface gas will remain molecular but be heated to peak temperatures of 10^3-2×10^3 K. Since the Jeans length at the highest temperatures is much greater than the thickness of the hottest zone in the interface, stars would not be expected to form until the post-shock gas has cooled to approximately 100 K. At that point, the highest mass stars will form first in the cooling gas, thus favoring massive stars in the initial mass function.

The mechanism of cloud-cloud collisions to form OB stars is consistent with a number of previous observations of OB star formation. Most important

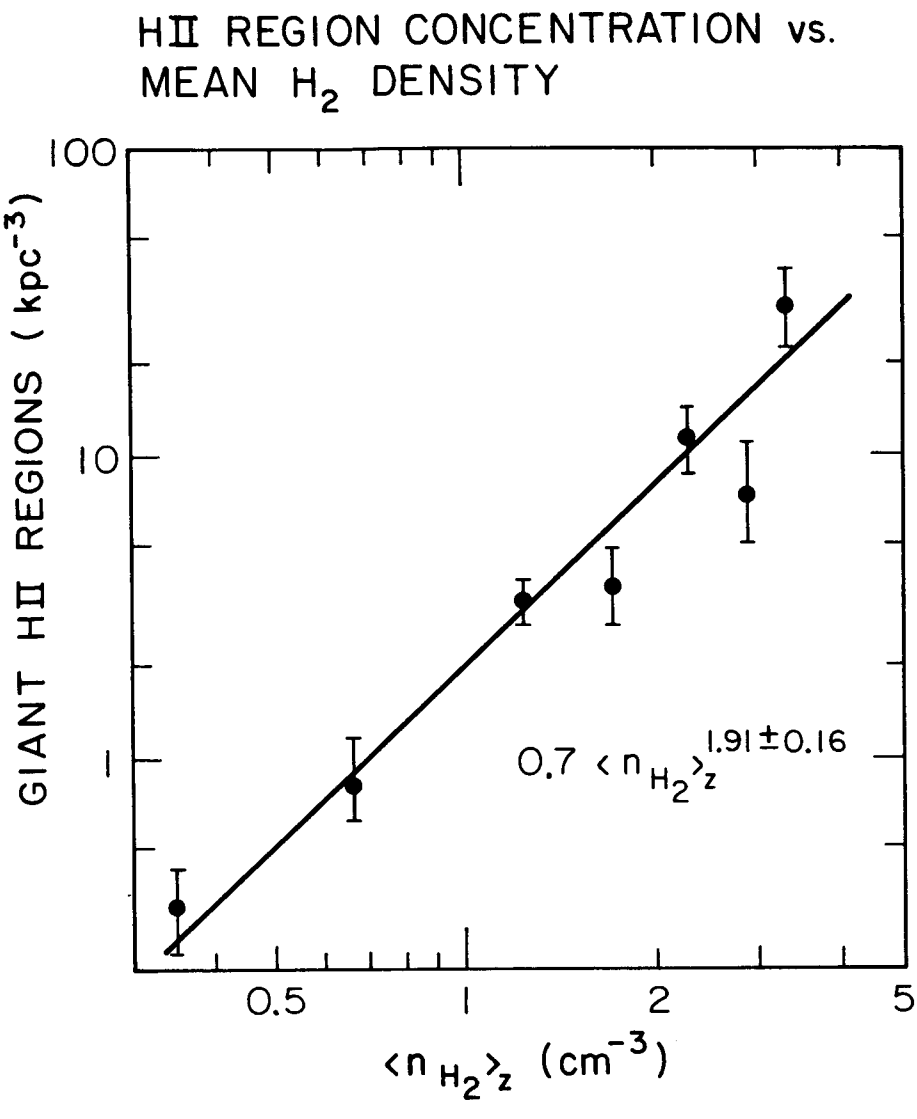

Figure 4. The number density of HII regions depends quadratically on the local H_2 density (averaged over ∿300 pc in the galactic plane). The face-on density of H_2 is taken from Clemens, Sanders, and Scoville (1986).

is the fact that one may now understand the concentration of HII regions along the spiral arms as resulting from the convergence of cloud orbits in the spiral potential minimum associated with the density wave. With a modest 5% spiral perturbation, Kwan and Valdes (1983) found that the number density of clouds increased by a factor of approximately three in the spiral arms which would result in an increase of the collision rate by a factor of nine. This corresponds well to the observed contrast between arm and interarm HII regions -- Mezger and Smith (1977) find 15% of the giant HII regions in classic interarm areas of the l-V plane. In addition, it has often been noted that OB star formation occurs with a low duty cycle in molecular clouds, that is, the time during which massive star formation occurs is relatively short compared to the spread of ages for lower mass young stars within the clouds. In the collision model,

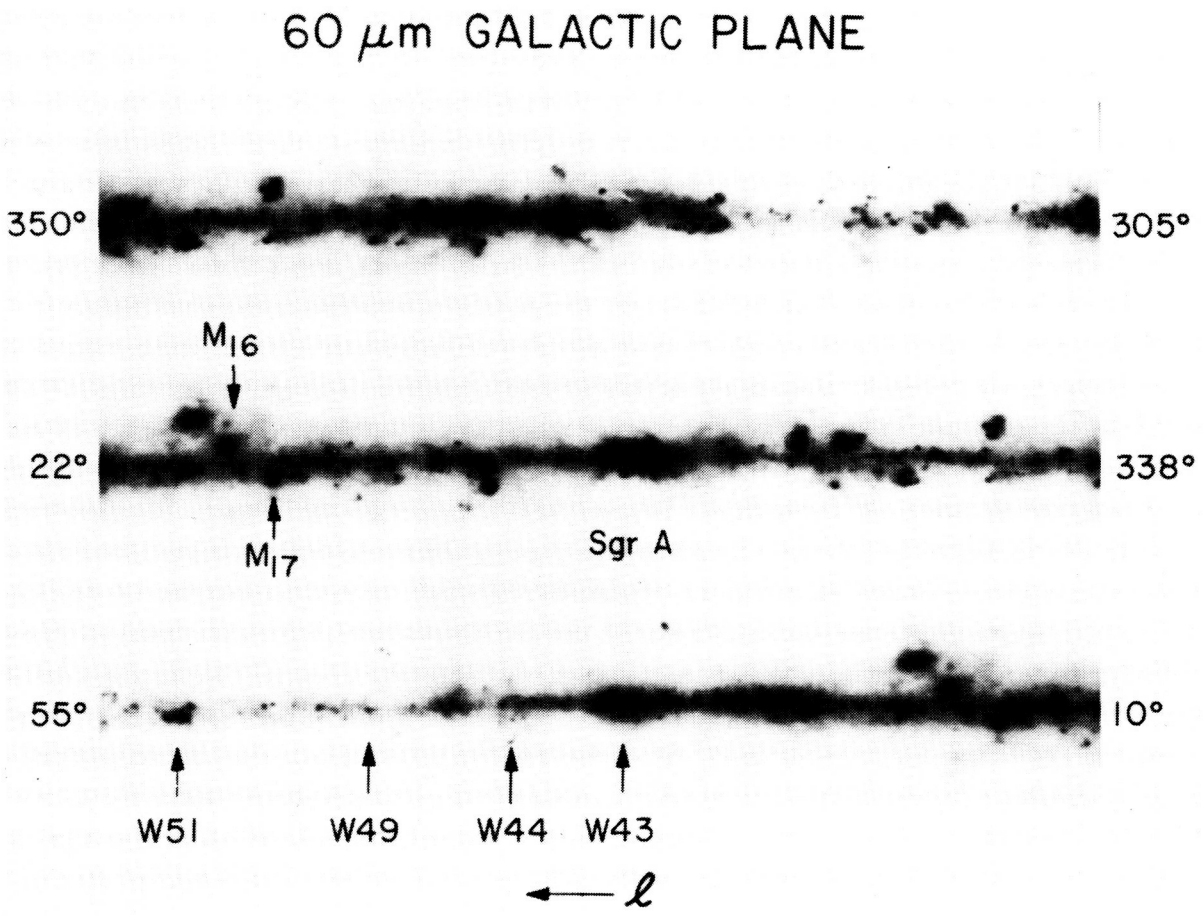

Figure 5. The 60 μm IRAS data were used to produce a constant, logarithmic stretch image of the first galactic quadrant. The image was prepared at IPAC by G. Laughlin.

it is natural to expect a low duty cycle as a result of the fact that the cloud crossing time (that is, the interaction time) is a factor of 5-10 less than the mean time between cloud collisions.

The HII regions formed during cloud collisions could be found deep in the cloud interior or near the edge of the merged cloud, depending on the relative masses of the initial two clouds. Since the largest fraction of the gas will be activated in collisions of equal mass clouds, one would also naturally predict a peak OB star formation efficiency (per mass of H_2 gas) at intermediate cloud masses. Finally, we note that the resulting HII regions will line up along the collision interface; thus, the model will be consistent with all the observational evidence which has been summoned to support sequential star formation models (cf. Elmegreen and Lada 1977).

5. THE INFRARED EMISSION ASSOCIATED WITH MOLECULAR CLOUDS

As a result of the IRAS survey, there now exists reasonably complete spectral

and spatial information for the infrared emission associated with the GMCs detected in the Massachusetts-Stony Brook CO survey. Identification of discrete CO emission complexes with concentrations of far infrared emission in the IRAS survey also enables us to determine the kinematic distances for numerous far infrared sources and thus to estimate luminosities from the IRAS flux measurements. Figure 5 is a far infrared image of the first galactic quadrant constructed from the 60 μm data with a constant logarithmic stretch. Each of the three strips contains 10° of latitude and 45° of longitude.

5.1 The Total Far Infrared Luminosity From Molecular Clouds

In Figure 6, we compare the longitude distributions of the far infrared luminosity, molecular hydrogen mass, and dust temperature (derived from the 60 and 100 μm fluxes with a dust emissivity $\propto \lambda^{-1}$, see Appendix B of Lonsdale et al 1985). For both the CO and IRAS data, the fluxes were averaged over a window of $\Delta b=2°$ and $\Delta l=2.5°$, and in the infrared, a background was subtracted corresponding to the fluxes at $b=\pm 1°$. The far infrared luminosity includes the bolometric correction for λ=1-500 μm (Lonsdale et al 1985). For both the H_2 mass and the infrared luminosity, the units are displayed in solar units for a reference distance of 1 kpc. Since the bulk of the emission in the range $l=10-50°$ arises from regions at a distance of 5-15 kpc, the vertical scale should generally be multiplied by factors of 25-225.

The dominant feature in both the CO and far infrared luminosity distributions is the molecular ring at $l=20-50°$. For the range $l=8-50°$ the mean ratio of l_{IR}/m_{H_2} is 2.75 L_o/M_o and the mean far infrared dust temperature is 29.3 K. There are, however, very notable departures from a constant IR:CO ratio in the vicinity of high luminosity HII region complexes, for example, at l=24, 34, 50 and 75°.

Assuming that, on average, the far infrared emission arises with the same distribution of source distances as the CO, we may use existing CO mass estimates to derive the total far infrared luminosity of molecular clouds in the galactic plane. That is, global models for the CO emission distribution in the galactic disk (for which the source distances were derived from the CO velocities and scale heights) may be applied directly to yield the d^2 factors needed to convert the far infrared fluxes in Figure 6 into luminosities. For a solar distance of 8.5 kpc, Clemens, Sanders, and Scoville (1986) deduce a molecular mass of 2.1×10^9 M_o for the region R>1.5 kpc. Using the mean ratio of far infrared luminosity to CO mass (2.75 L_o/M_o), we obtain a total far infrared luminosity from the same region of 5.8×10^9 L_o.

The luminosity in the galactic center region may be estimated directly from the observed flux assuming that all of the radiation observed at l=-2.5 to +2.5° originates at a distance of 8.5 kpc. The luminosity from this region, corresponding to $R\leq 375$ pc, is 7×10^8 L_o.

It should be noted that this luminosity estimate does not include emission components with large latitude thickness since we removed the "background" flux at $b=\pm 1°$. Although part of the emission which varies slowly in latitude is undoubtedly local and therefore does not represent a significant addition to the overall Galactic luminosity, some of the high latitude emission must originate in the 3-7 kpc ring on the basis of the longitude variation which shows a maximum

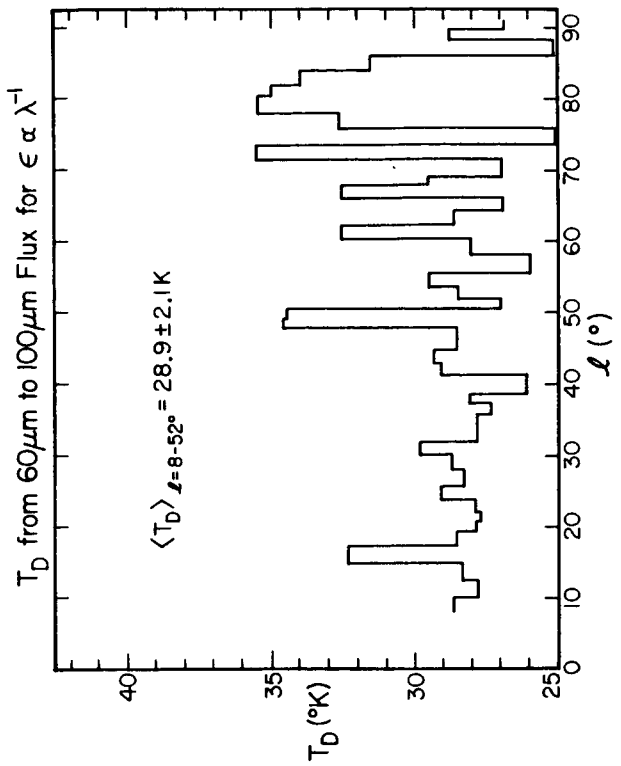

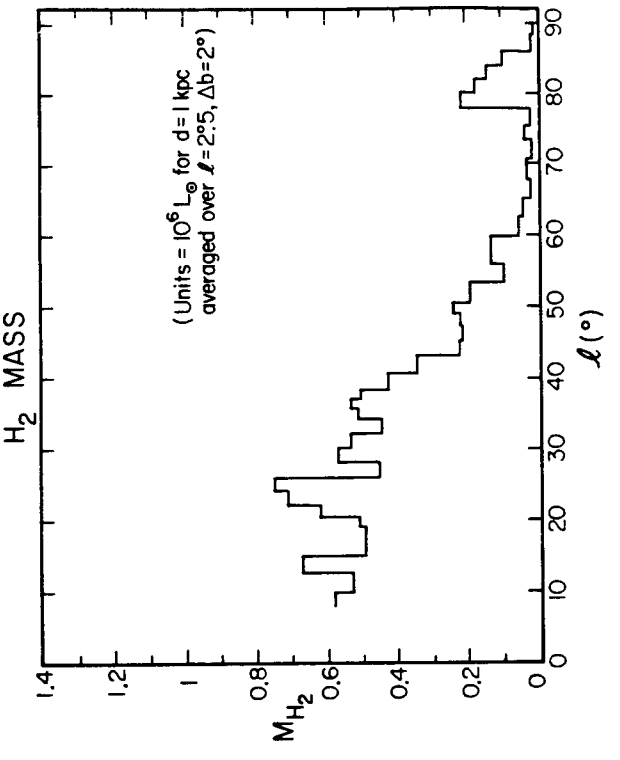

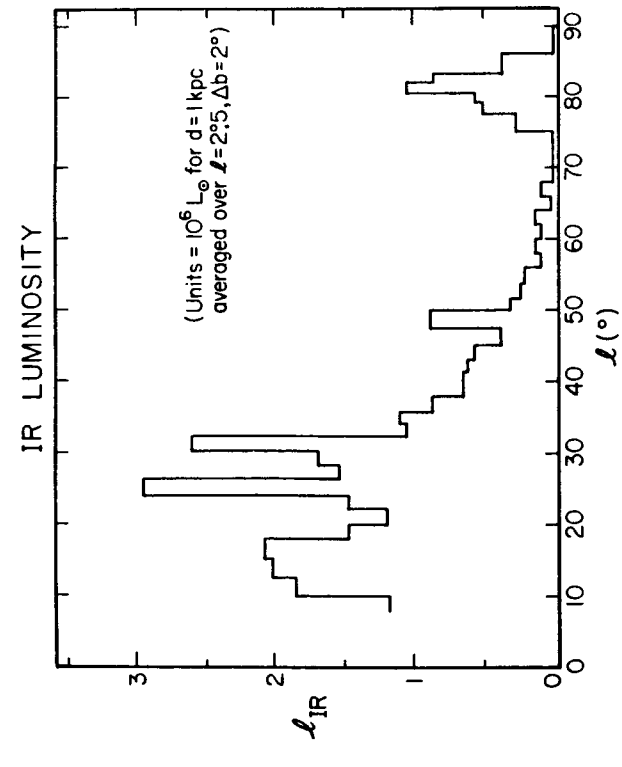

Figure 6. The longitude distribution of far infrared luminosity (λ=1-500 μm), dust temperature, and H_2 mass density are shown as averaged over a 2°x2°.5 (Δb x Δl) window. The dust temperature and luminosity was calculated from the 60 and 100 μm data assuming a dust emissivity $\varepsilon_\lambda \propto \lambda^{-1}$.

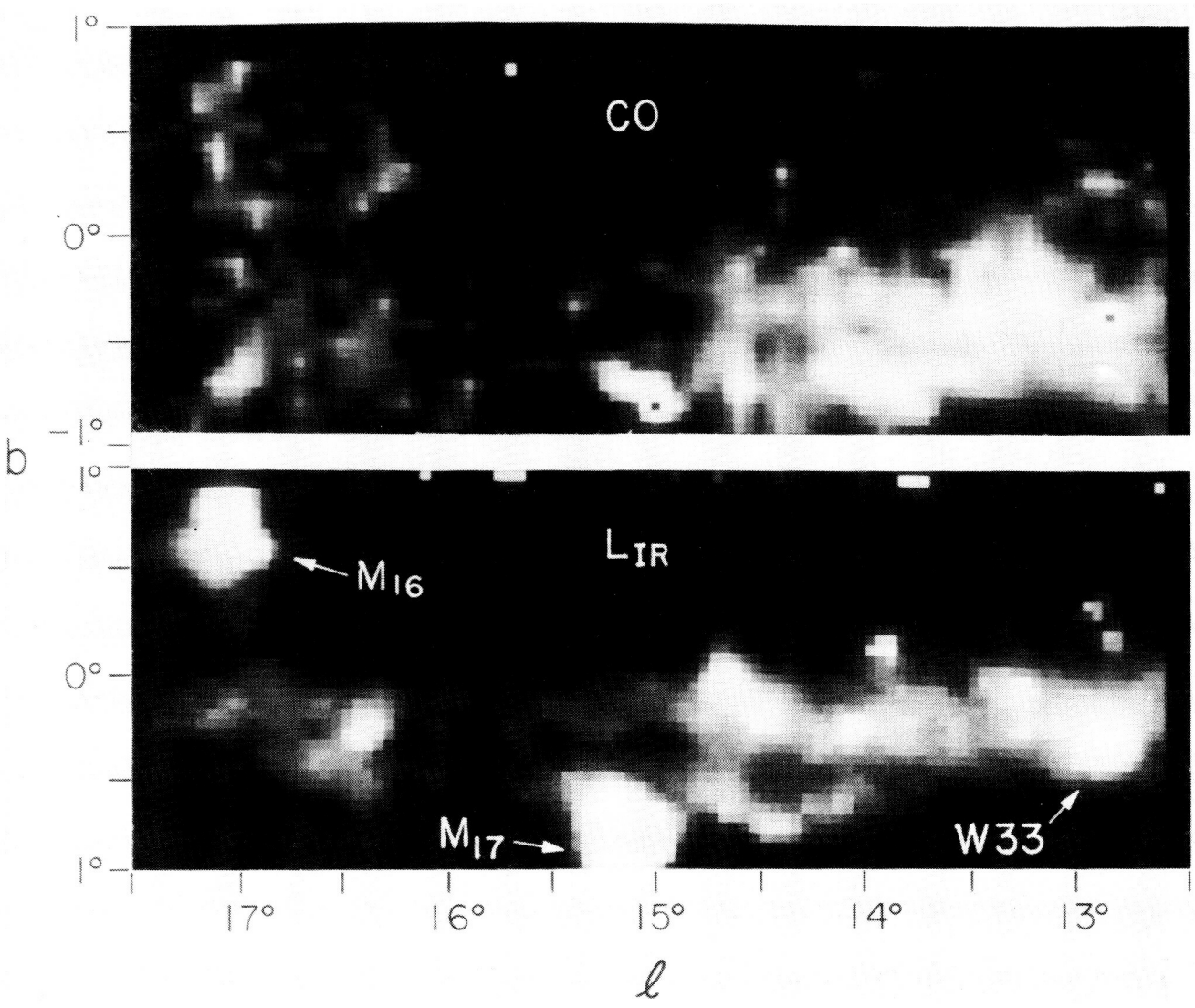

Figure 7a. The far infrared luminosity (λ=1-500 μm) and CO (V=10->40 km s^{-1}) distributions are shown for a 2x5° area of the galactic plane including M16 and M17. Pixels are 3x3'.

in the range l=20-50° (Puget et al 1986). This diffuse component could constitute as much as 50% of the total far infrared luminosity. Although the emission, seen at $|b|>1°$, is probably emitted by dust associated with non-molecular ISM, the energy sources of this luminosity are presumably situated closer to the galactic plane in the molecular cloud ring.

5.2 The Infrared Luminosity of Individual Clouds

In Table 1, the far infrared and CO properties are summarized for GMCs associated with the high luminosity HII regions M17, M16 and W51. Measurements are given for regions of varying diameter in each cloud -- including both the primary infrared sources associated with the HII regions and the more extended

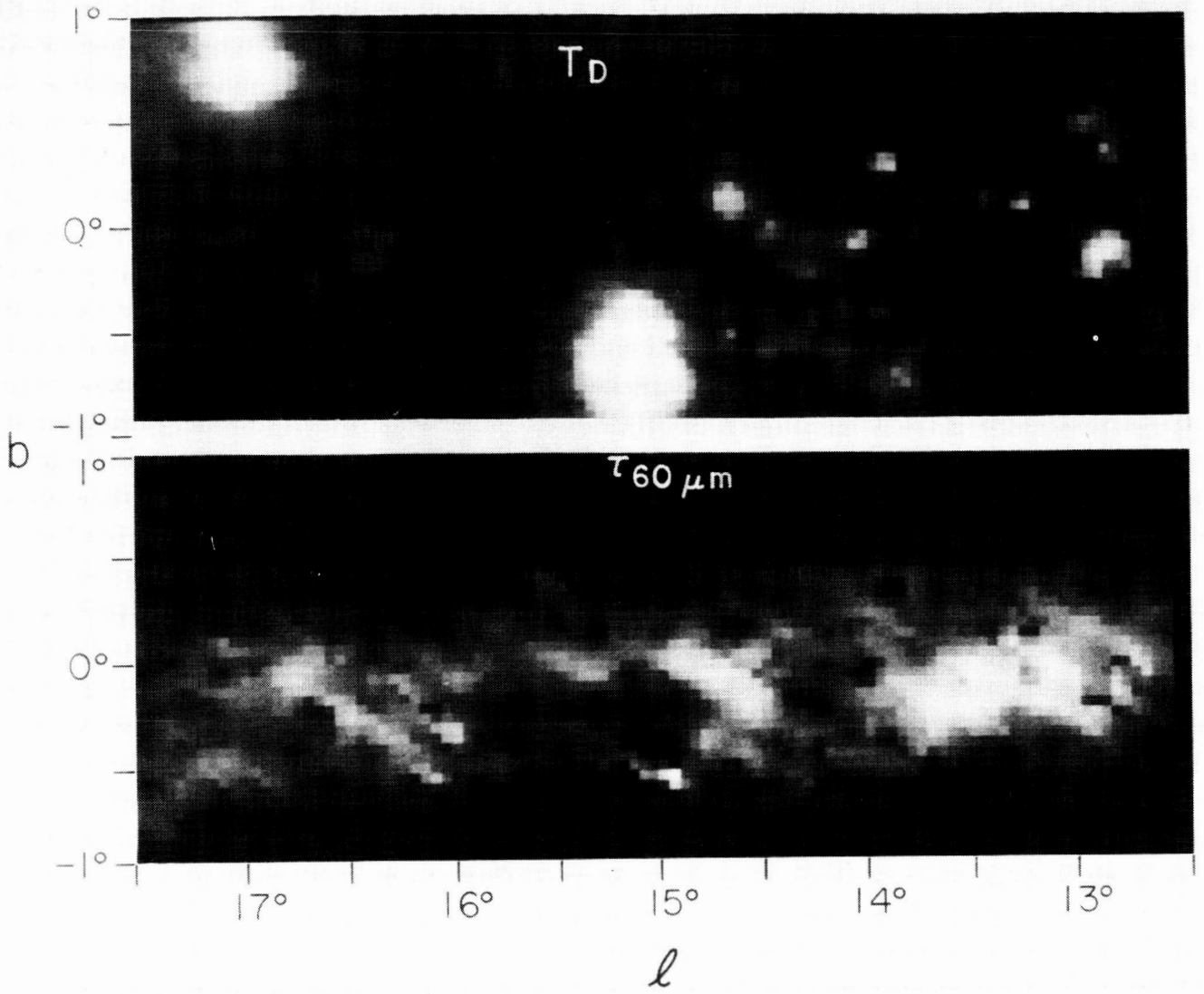

Figure 7b. The far infrared optical depth and dust temperature maps are shown for the same area as Figure 7a including M16 and M17. The opacity and temperatures were derived from the 60 and 100 μm IRAS data following the prescription given by Lonsdale et al (1985) for $\varepsilon_\lambda \propto \lambda^{-1}$. The image stretch is $\tau_{60\ \mu m}$=0-0.5 and T_D=25-45 K.

emission associated with the much larger molecular clouds.

The ratio of far infrared luminosity to molecular mass is a factor of ten higher than the galactic plane average of l_{IR}/m_{H_2}=2.75 L_o/M_o in the immediate vicinity of the luminous HII regions. The maximum value for L_{IR}/M_{H_2} (25.7 L_o/M_o) is obtained on M16. It is noteworthy that even though the ratio of far infrared luminosity to H_2 mass decreases as one includes larger areas of the cloud, inclusion of the entire GMC (100 pc in diameter) still yields a high L_{IR}/M_{H_2} ($\sim$10 L_o/M_o) which is much greater than the mean value obtained for the galactic plane.

Images of the CO and far infrared emission in a 2x5° (bx1) area of the

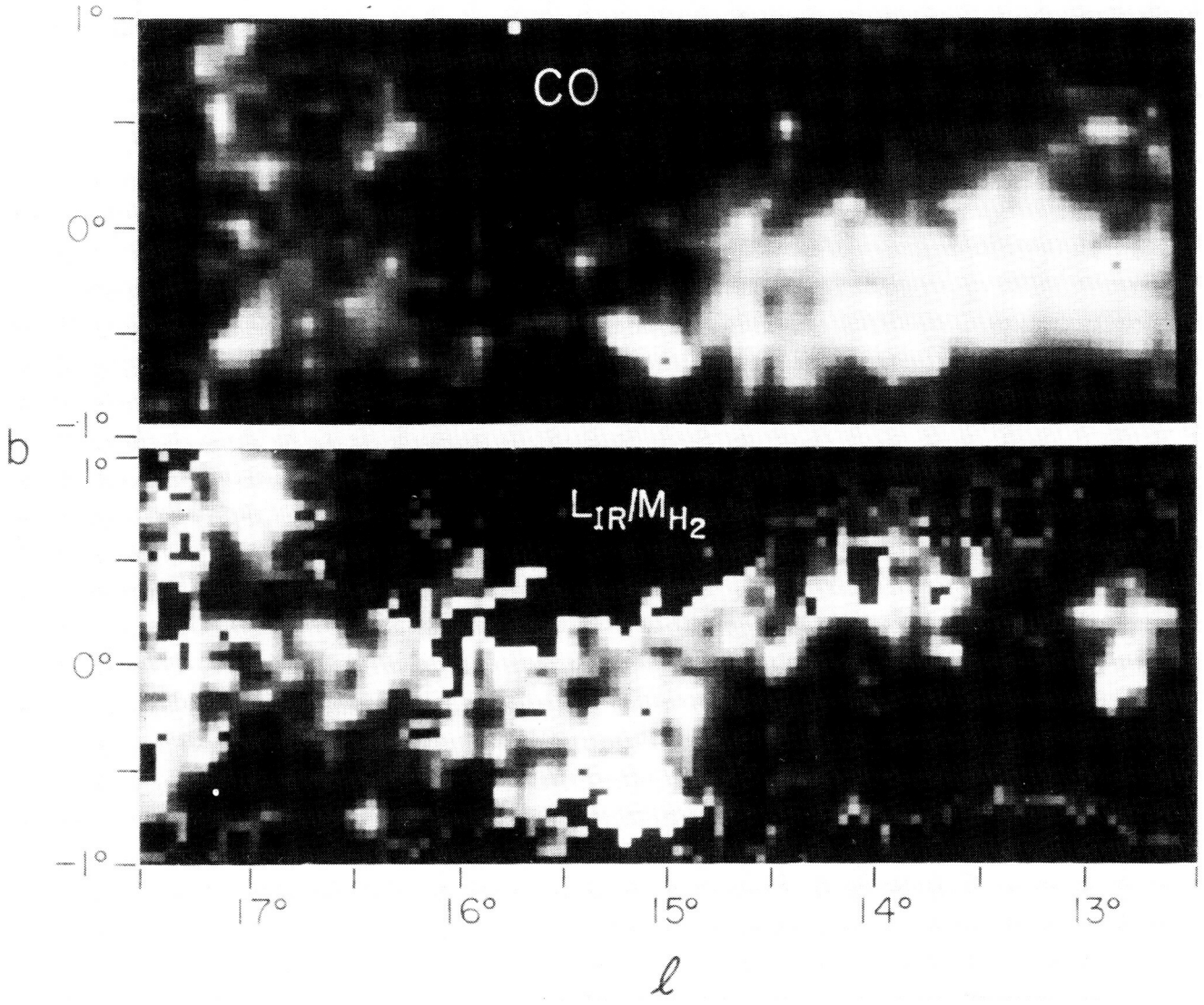

Figure 7c. The CO and L_{IR}/M_{H_2} maps for M16 and M17. The stretch for L_{IR}/M_{H_2} is from 3 to 30 L_o/M_o and the image is blanked where the CO measurement is less than 7σ.

galactic plane including M16 and M17 are shown in Figure 7. The CO emission was integrated from V_{LSR}=-10 to 40 km s^{-1} and the infrared optical depth, dust temperature and luminosity were computed assuming an emissivity $\varepsilon_\lambda \propto \lambda^{-1}$ (see Lonsdale et al 1985). The infrared emission in the vicinity of the HII regions is characterized by low opacity, high temperature and high luminosity density. In areas of the GMCs away from the HII regions, the dust appears significantly colder than even the galactic background and hence, the GMCs show up on the dust temperature map as dark areas (which also have high opacity). The L_{IR}/M_{H_2} map clearly shows the tendency for high values in the vicinity of the HII regions and in general along the cloud boundaries where the interstellar uv probably heats the peripheral dust.

Table 1

IR Properties of High Mass Star Formation Regions[a]

Region	Diameter (pc)	M_{H_2}[b] ($M_\odot$)	L_{IR}[b] ($L_\odot$)	L_{IR}/M_{H_2} ($L_\odot/M_\odot$)	IRE[b]	T_D (K)
M16	20	9×10^4	1.3×10^6	15	14	36
M17	18	9×10^4	3.4×10^6	37	2.4	43
	75	1×10^6	1.3×10^7	13	6.9	31
W51	50	8.7×10^5	1.3×10^7	15	4	39
	135	2.8×10^6	2.7×10^7	9.6	6.9	35
Galactic Center[c]	740	2×10^8	6.8×10^8	3.5		31
Galactic Disk[d]		2.2×10^9	6×10^9	2.8		29

Notes

a) Assumes R_o=8.5 kpc throughout.

b) M_{H_2} evaluated from $N_{H_2}=3.6\times10^{20}$ H_2 cm^{-2} (K km $s^{-1})^{-1}$ (Scoville et al 1986). L_{IR} obtained from 60 and 100 μm IRAS fluxes with an assumed λ^{-1} emissivity law (see Appendix B of Lonsdale et al 1985). The infrared excess (IRE) was evaluated from L_{IR} and the radio free-free flux (cf. Myers et al 1986).

c) l=-2°.5 to +2°.5, b=-1° to +1°. The IR background at $|b|=1°$ was removed.

d) R<1.5 kpc. The IR galactic background at $|b|=1°$ was removed.

6. APPLICATION TO HIGH LUMINOSITY IRAS GALAXIES

Recently, Sanders et al (1986) have obtained single dish CO measurements for some of the distant IRAS galaxies. Their results indicate typical L_{IR}/M_{H_2} ratios in the range 10-50. These values are generally consistent with those obtained for Galactic GMCs associated with HII regions (Table 1), suggesting that high mass star formation is a viable energy source in the luminous IRAS galaxies. However, it is then required that virtually all the clouds in these galaxies have conditions similar to the most active areas in W51 and M17 and this may be somewhat implausible.

With regard to the suggestion by Scoville, Sanders and Clemens (1986) that most massive star formation in our own galaxy results from cloud-cloud collisions, it is noteworthy that Sanders et al (1986) have found that the majority of the distant high luminosity IRAS galaxies are in fact interacting galaxy pairs in which one would expect a high frequency of collisions between the interstellar clouds of the two galaxies.

We acknowledge support for this work under the IRAS General Investigator Program (NS) and NSF Grant AST 84-12473.

7. REFERENCES

Allen, R.J., Atherton, P.D., and Tilanus, R.P.J. 1986, Nature, **319**, 296.
Burton, W.B. and Gordon, M.A. 1978, Astron. Astrophys., **63**, 7.
Burton, W.B., Gordon, M.A., Bania, T.M., and Lockman, F.J. 1975, Ap.J., **202**, 30.
Clemens, D.P. 1985, Ap.J., 295, 422.
Clemens, D.P., Sanders, D.B., and Scoville, N.Z. 1986, Ap.J. (submitted).
Cohen, R.S., Cong, H., Dame, T.M., and Thaddeus, P. 1980, Ap.J. (Letters), **239**, L53.
Cohen, R.S., Tomasevich, G.R., Thaddeus, P. 1979, in IAU Symposium 84, The Large Scale Characteristics of the Galaxy, ed. W.B. Burton (Dordrecht: Reidel), p.53.
Downes, D., Wilson, T.L., Bieging, J., and Wink, J. 1980, Astr. Ap. Suppl., **40**, 379.
Elmegreen, B.G. and Lada, C.J. 1977, Ap.J., **214**, 725.
Herbst, W. and Assousa, G.E. 1977, Ap.J., **217**, 473.
Kwan, J. and Valdes, F. 1983, Ap.J., **271**, 604.
Lockman, F.J. 1986 (in preparation).
Lonsdale, C.J., Helou, G., Good, J.C., and Rice, W.L. 1985, Catalogued Galaxies and Quasars Observed in the IRAS Survey (Washington : U.S. Government Printing Office).
Myers, P.C., Dame, T.M., Thaddeus, P., Cohen, R.S., Silverberg, R.F., Dwek, E., and Hauser, M.G. 1986, Ap.J., **301**, 398.
Mezger, P.G. and Smith, L.F. 1977, Star Formation, IAU Symposium No. 75, ed. de Jong, T. and Maeder, A., (Dordrecht: Reidel), p. 133.
Puget, J.L., Falgarone, E., Perault, M., and Ryter, C. 1986, in Star Formation in Galaxies, ed. C. Persson.
Robinson, B.J., Manchester, R.N., Whiteoak, J.B., Sanders, D.B., Scoville, N.Z., Clemens, D.P., McCutcheon, W.H., and Solomon, P.M. 1984, Ap.J. (Letters), **283**, L31.

Rydbeck, G., Hjalmarson, A., and Rydbeck, O.E.H. 1985, Astron. Astrophys., **144**, 282.
Sanders, D.B. 1981, Ph.D. thesis, State University of New York at Stony Brook.
Sanders, D.B., Clemens, D.B., Scoville, N.Z., and Solomon, P.M. 1986, Ap.J. Suppl., **60**, 1.
Sanders, D.B., Scoville, N.Z., and Solomon, P.M. 1985, Ap.J., 289, 373.
Sanders, D.B., Scoville, N.Z., Young, J.S., Soifer, B.T., Schloerb, F.P., Rice, W.L., and Danielson, G.E. 1986, Ap.J. (Letters), **305**, L45.
Sanders, D.B., Solomon, P.M., and Scoville, N.Z. 1984, Ap.J., **276**, 182.
Scoville, N.Z. and Sanders, D.B. 1986, in Interstellar Processes, ed. Thronson, H. and Hollenbach, D. (Dordrecht: Reidel) (in press)
Scoville, N.Z., Sanders, D.B., and Clemens, D.P. 1986, Ap.J. (Letters), (November 15).
Scoville, N.Z. and Solomon, P.M. 1975, Ap.J. (Letters), **199**, L105.
Scoville, N.Z., Yun, M.S., Clemens, D.P., Sanders, D.B., and Waller, W.H. 1986, Ap.J. Suppl. (submitted).
Solomon, P.M., Sanders, D.B., and Rivolo, A. 1985, Ap.J. (Letters), **292**, L19.

DISCUSSION

ELMEGREEN:

Molecular clouds are clumpy and stars form in the dense clumps. The average density in cloud complexes decreases with increasing cloud mass, so the star-forming cores represent a smaller and smaller fraction of the overall cloud mass as this overall mass increases. This may explain why the efficiency decreases with increasing mass; this decrease may be independent of sequential star formation processes. The observed clumpiness also explains the low star formation efficiency without the need for physical assumptions about cloud stability. The clumps dissipate their kinetic energy in only several crossing times and eventually form cores dense enough for star formation. The efficiency in these cores can be large (10%-50%), but the overall efficiency in the whole cloud, low. Cloud complexes need not be 'stable' for any longer time than this clump dissipation time. Star formation is not necessarily the same as clump formation because the clumps could be primordial, that is, the big clouds may form by a coalescence of smaller clouds, which are still visible as clumps.

SCOVILLE:

If the decreased efficiency for massive star formation in higher mass clouds is the result of the decreased fraction of the cloud mass in dense clumps, then this also implies that 'sequential star formation' has little to do with the OB star formation i.e., the formation of massive stars is simply due to the pre-existing clump structure in the clouds. In any case, there are as yet no observational studies suggesting that the fraction of mass in dense clumps is any different in high-mass clouds than in low-mass clouds. The mean density is probably higher in the latter case, but it does not follow that this is the result of a higher clump fraction.

HUNTER:

You have said that galaxies with low 'CO contents' would preferentially form low-mass stars. What about irregular galaxies which have low CO luminosities and yet plenty of high-mass star formation?

SCOVILLE:

The critical factor is not the absolute 'CO content' but rather the concentration of the molecular gas. You could certainly have situations in which the overall molecular gas content of a galaxy was low but the clouds were restricted to a small region (or had a high velocity dispersion) so that the frequency of cloud-cloud

collisions was high, resulting in a high rate of OB star formation. One should also note that massive star formation in the irregular galaxies with low H_2/HI ratios could result from collision of HI clouds.

HUNTER:

But in NGC 4449, for example, the high mass star formation is scattered throughout the galaxy, so clouds would have to be colliding over the entire disk. This implies a lot of molecular mass.

BEGELMAN:

Is there actually time for gravitational collapse to occur at the cloud-cloud interface during the collision? Even if cooling is very rapid, collapse can occur no faster than the free-fall time. In the limit of rapid cooling, the interface would cool isochorically rather than isobarically.

SCOVILLE:

Depending on the size of the GMCs undergoing a collision, the collision time could be up to 10^7 years which is much greater than the 10^6 year free-fall time at density $\geq 10^3$ cm^{-3}.

ELIAS:

With regard to the point about HII regions being at the center of molecular clouds, I noticed, first, that the specific examples you showed had the HII region toward the edges, and, second, that the clouds were very non-spherical. How does this affect your statistical discussion?

SCOVILLE:

I agree that the interpretation of the HII region offsets is very dependent on the assumed geometry of the clouds, i.e., whether they are spherical or elongated.